Dislocation Evolution in Metals During Irradiation

W.G. Wolfer and B.B. Glasgow

October 1984

UWFDM-602

Submitted to Acta Met.

FUSION TECHNOLOGY INSTITUTE

UNIVERSITY OF WISCONSIN

MADISON WISCONSIN

"LEGAL NOTICE"

"This work was prepared by the University of Wisconsin as an account of work sponsored by the Electric Power Research Institute, Inc. ("EPRI"). Neither EPRI, members of EPRI, the University of Wisconsin, nor any person acting on behalf of either:

"a. Makes any warranty or representation, express or implied, with respect to the accuracy, completeness, or usefulness of the information contained in this report, or that the use of any information, apparatus, method, or process disclosed in this report may not infringe privately owned rights; or

"b. Assumes any liabilities with respect to the use of, or for damages resulting from the use of, any information, apparatus, method or process disclosed in this report."

Dislocation Evolution in Metals During Irradiation

W.G. Wolfer and B.B. Glasgow

Fusion Technology Institute
University of Wisconsin
1500 Engineering Drive
Madison, WI 53706

http://fti.neep.wisc.edu

October 1984

UWFDM-602

Submitted to Acta Met.

DISLOCATION EVOLUTION IN METALS DURING IRRADIATION

W.G. Wolfer and B.B. Glasgow

Fusion Technology Institute
Nuclear Engineering Department
University of Wisconsin-Madison
Madison, Wisconsin 53706

October 1984

UWFDM-602

*Submitted to Acta Met.

DISLOCATION EVOLUTION IN METALS DURING IRRADIATION[†]

W.G. Wolfer and B.B. Glasgow

Fusion Technology Institute and Department of Nuclear Engineering
University of Wisconsin, Madison, WI 53706 USA

ABSTRACT

Physical models are developed for the evolution of the dislocation density in metals subject to irradiation at elevated temperatures. Two basic processes are shown to account for the experimental observations: the generation of dislocation line length takes place by the Bardeen-Herring mechanisms, whereas dislocation loss can be described in terms of dislocation dipole annihilation. Only two microstructural parameters, namely the mesh length and the bias variance, need to be introduced and adjusted in order to reproduce the experimental observations on dislocation evolution in type austenitic stainless steels.

[†]This work has been supported by the Electric Power Research Institute, Palo Alto, under contract RP1597-2 with the University of Wisconsin.

1. INTRODUCTION

During the bombardment of metals with energetic particles, vacancies and self-interstitials are produced. At irradiation temperatures above the onset for vacancy migration but below the temperature where self-diffusion is rapid, the absorption of vacancies and interstitials at dislocations leads eventually to dramatic changes of the dislocation density. Other microstructural defects also arise, such as small dislocation loops, voids, and precipitates as a result of the irradiation. However, the evolution of the dislocation density is nearly independent of the evolution of all other microstructural features. Well-annealed metals exhibit a sharp increase with irradiation dose of the dislocation density which eventually approaches a saturation value. In cold-worked metals, however, the dislocation density drops with dose and approaches a saturation value similar or even identical to the one in the well-annealed counterpart. The observation that this saturation value is independent of the initial dislocation density has led several researchers [1-3] to suggest that the evolution of the dislocation network is the result of two competing processes, namely the generation of dislocations by loop growth and by the climb of edge dislocations and the mutual annihilation of dislocations with opposite Burgers vectors.

These general ideas [2,4] provided the background for the empirical models of dislocation evolution proposed earlier, according to which the rate of change of the dislocation density $\rho(t)$ is given by

$$\frac{d\rho}{dt} = B\rho^m - A\rho^n \quad . \tag{1}$$

The logical choice for n is two since the annihilation of dislocations in-

volves pairs with opposite Burgers vectors. For the production term, a plausible choice would be m = 1. However, Garner and Wolfer [4] provided heuristic arguments for n = 3/2 and m = 1/2. Unfortunately, the experimental data for $\rho(t)$ are not sufficiently accurate to determine the exponents m and n, and the choice of m = 1 and n = 2 appears to give an equally satisfactory correlation [2]. The question of the correct exponents must therefore be answered by developing concrete physical models for both the production and the annihilation term. This will be the main purpose of the present paper. A review of the experimental results has been given earlier [4], and any discussion of those will be postponed to Section 5 where the measured dislocation densities are then compared with the theoretical predictions. Preceding this comparison, a model for the annihilation or recovery term $A\rho^2$ will be derived in Section 2, and Section 3 will deal with the derivation of the dislocation generation term $B\rho$. It will be found that both A and B are dependent on the dislocation density $\rho(t)$. Both processes require the climb motion of edge dislocations as a result of either an excess of self-interstitial absorption, or an excess of vacancy absorption or emission. At temperatures below about half of the melting point, the necessary climb motion can occur only if sinks with different point defect biases are present in the microstructure, where the bias is a measure of the preferential absorption of interstitials. Accordingly, we discuss in Section 4 the need and the extent of the bias variance necessary for the evolution of the dislocation structure to occur under irradiation. The comparison of the theory with the experimental data in Section 5 is limited to austenitic stainless steels irradiated in fast-neutron reactors, because the experimental irradiation conditions are well characterized, and the effects of the specimen surface are negligible. For irradi-

ations performed with ion bombardment or electron beams, several additional complications exist such as a non-uniform defect production and a significant loss of dislocations to both the surface [3] and the portion of the specimen [5] not subject to radiation damage. For the present model to be applicable for ion bombardment or electron irradiations, these additional aspects must be included. However, they add little to the elucidation of the basic mechanisms which control the evolution of the dislocation density during high-temperature irradiations, and they will not be dealt with in this paper.

2. DISLOCATION RECOVERY

The reduction of the dislocation density in cold-worked metals by annealing involves the thermally activated climb of dislocations and the mutual annihilation of dislocations in dipole configurations. It is reasonable to assume then that the process of dipole annihilation takes place also under irradiation, and that this process is enhanced as a result of the radiation-induced climb. In the following, an edge dislocation dipole is considered to consist of two nearly parallel segments of edge dislocations with parallel or anti-parallel Burgers vectors. The segment can either belong to line dislocations or to dislocation loops with a diameter significantly greater than the distance between the dislocations in the dipole.

Among the four different dipole configurations, shown in Fig. 1, which have edge dislocations of parallel or anti-parallel Burgers vectors and whose glide planes are separated by a distance h, only one pair will converge to a common glide plane when either interstitials or vacancies are preferentially absorbed at edge dislocations. For this one pair, called the converging di-

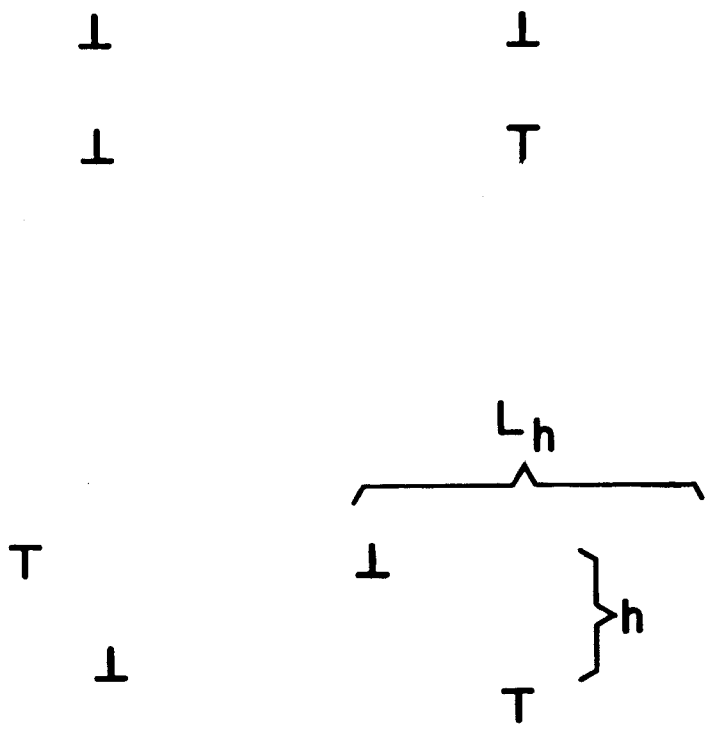

Fig. 1. Edge dislocation dipoles.

pole, h decreases with time, and if the segment can also glide under the mutual interaction force, annihilation will inevitably occur.

However, this requires that the interaction glide force overcomes a critical shear stress, τ_o. For a given τ_o this condition defines the maximum separation distance, h_{max}, from which a converging dipole may form. Using the glide force for an edge dislocation dipole [6], we obtain

$$\frac{\mu b}{2\pi(1 - \nu)h_{max}} = \tau_o \ , \tag{2}$$

where b is the Burgers vector, μ the shear modulus, and ν Poisson's ratio.

In alloys such as steels, dislocation motion is restricted by glide obstacles such as precipitates and by forest dislocations. Dislocation glide requires then the activation of Frank-Read sources. Accordingly, we assume that the critical shear stress τ_o for the glide motion of a dislocation segment is well approximated by the condition for the activation of a Frank-Read source of length ℓ [6], i.e.

$$\tau_o = \frac{\mu b}{2\pi(1 - \nu)\ell} \ln \left(\frac{\ell}{b}\right) . \tag{3}$$

Equations (2) and (3) define then the maximum separation distance h_{max} unless the dislocation density is so high that the average distance between parallel dislocation segments is less than this value.

Since $\rho/12$ is the dislocation density belonging to one glide system in the fcc lattice, and since only one pair out of four will form a converging dipole, the average separation distance is $8/\sqrt{\pi\rho/3}$ between those dislocation segments capable of forming such a dipole. Hence,

$$h_{max} = \text{Min}\ \{8/\sqrt{\pi\rho/3}\ ,\ \ell/\ln\ (\ell/b)\}\ . \tag{4}$$

Let us assume now that at any given moment, the total number of all converging dipoles with a separation distance of their glide planes between h and h + dh and with a separation distance parallel to the glide planes of $L_h/2$ or less (see Fig. 1) is given by $12\ \frac{1}{4}\ (\rho/12)^2\ L_h\ dh$ for a given glide system. If $h \leq h_{max}$, the dipole will in fact assume a configuration close to its mechanical equilibrium and $L_h \cong 2h$. Furthermore, let $\tau(h)$ denote the lifetime of a converging dipole of initial separation h. Then the rate of dislocation annihilation is finally given by

$$A\rho^2 = \frac{1}{24}\ \rho^2 \int_b^{h_{max}} \tau^{-1}(h) h\ dh \tag{5}$$

where we have summed over all 12 glide systems, but divided by four because three out of four dipole configurations are not converging.

If V(h) represents the climb velocity of one dislocation, then the converging dipole lifetime is

$$\tau(h) = \int_b^h dh'/2V(h')\ . \tag{6}$$

The climb velocity

$$V(h) = \frac{\Omega}{\hbar}\ [Z_i^d D_i C_i\ -\ Z_v^d D_v C_v\ +\ Z_v^d D_v C_v^d(h)\ ] \tag{7}$$

is determined by the concentrations of vacancies, C_v, and interstitials, C_i, by their diffusion coefficients, D_v and D_i, and by the vacancy concentration,

$C_v^d(h)$, in local thermodynamic equilibrium with the dislocation. According to Kroupa [7]

$$C_v^d(h) = C_v^{eq} \exp\left(\frac{Hb}{h}\right) \tag{8}$$

where C_v^{eq} is the equilibrium vacancy concentration in the defect-free lattice,

$$H = \frac{\mu\Omega}{2\pi(1-\nu)kT}, \tag{9}$$

Ω is the atomic volume, and kT has the usual meaning. The concentrations C_v and C_i can be obtained from two rate equations discussed in the Appendix, and V(h) can be written as

$$\begin{aligned} V(h) &= \frac{\Omega}{b}\left[\frac{Z_i^d}{Z_v^d} - \frac{\bar{Z}_i}{\bar{Z}_v}\right] Z_v^d D_v \Delta C_v + \frac{\Omega}{b} D_v Z_v^d C_v^{eq} \left[\exp\left(\frac{Hb}{h}\right) - 1\right] \\ &= V_R + V_T \left[\exp\left(\frac{Hb}{h}\right) - 1\right]. \end{aligned} \tag{10}$$

The bias factors Z_i^d and Z_v^d contained in Eqs. (7) and (10) account for the effect of stress-induced migration on the absorption rate of interstitials and vacancies at edge dislocations, respectively. They are characteristic parameters of the type of sink under consideration.

Equation (10) shows that the climb velocity under irradiation can be separated into a radiation-induced part, V_R, and a thermally activated part proportional to V_T. The first part is proportional to excess vacancy concentration due to irradiation, ΔC_v, and the net bias, the expression in the

bracket. This net bias is only different from zero when the sink-averaged bias factors, $\bar{Z}_i$ and $\bar{Z}_v$, are different from the dislocation bias factors, Z_i^d and Z_v^d. This requires the presence of sinks other than dislocations. However, it will be shown in Section 4 that there exists a variance in the dislocation bias factors, and V_R will have to be modified. The modified V_R no longer vanishes when the sink structure consists only of dislocations.

With the expression for V(h), the dipole lifetime defined by Eq. (6) can now be evaluated. However, to obtain an analytical result, the following approximation must be made. Whenever the exponential term exp (Hb/h') is large, the climb velocity makes the least contribution to $\tau(h)$. Conversely, only for large values of h' will the thermally activated climb velocity contribute significantly to $\tau(h)$. In this case, exp (Hb/h') $\cong$ 1 + Hb/h' and

$$\tau(h) \cong \frac{1}{2} \int_b^h \frac{dh'}{(V_R + V_T Hb/h')} = \frac{h}{2V_R} - \frac{V_T Hb}{2V_R^2} \ln \left(1 + \frac{V_R h}{V_T Hb}\right) . \tag{11}$$

The coefficient A for the dislocation annihilation rate is then given by

$$A \cong \frac{1}{12} V_T Hb \int_{x_0}^{x_1} \left[1 - \frac{1}{x} \ln (1 + x)\right]^{-1} dx \tag{12}$$

where $x = V_R h/V_T Hb$, $x_0 = V_R/V_T H$, and $x_1 = V_R h_{max}/V_T Hb$. No closed-form solution to this integral could be found. However, two limiting cases can be evaluated easily. First, if $V_R >> V_T$, then $(1/x) \ln x << 1$, and

$$A \cong \frac{1}{12} V_R h_{max} \ . \tag{13}$$

Second, if $V_T >> V_R$, then $x << 1$, and we may expand $(1/x) \ln (1 + x) \cong 1 + x/2$ and also neglect V_R. In this case

$$A \cong \frac{1}{6} V_T Hb \ln (h_{max}/b) \ . \tag{14}$$

These two special cases represent the low- and high-temperature approximations, respectively. Because of the strong temperature dependence of self-diffusion, and hence of V_T, the range of temperatures, where V_R and V_T are of the same order, is very narrow. As a result, we may simply add the expressions and obtain the approximation

$$A \cong \frac{1}{12} V_R h_{max} + \frac{1}{6} V_T Hb \ln (h_{max}/b) \tag{15}$$

suitable for all temperatures. Note that V_R depends on the dislocation density $\rho(t)$.

3. DISLOCATION GENERATION

The dislocation density may increase during irradiation as a result of two processes. First, by the formation and growth of dislocation loops, and second, by the climb of dislocation segments pinned by obstacles. The latter process is exemplified by the Bardeen-Herring source [6].

Let us evaluate the average rate of increase for the dislocation density by these processes. Dislocation loops can grow under irradiation to an average maximum radius R_m, whereupon they may unfault and become part of the net-

work or coalesce with other loops or dislocations. If V represents then the mean climb velocity, the average lifetime of a dislocation loop is $\tau = R_m/V$. Assuming that $\bar{R} = R_m/2$ is the average loop radius at any instant, the dislocation density due to loops is $\rho = \pi R_m N_\ell$ averaged over a significantly large volume containing a density of N_ℓ loops.

The rate of increase of this dislocation density is then given by

$$B\rho = 2\pi R_m N_\ell/\tau = \rho V/\bar{R} \ . \tag{16}$$

To evaluate the change in dislocation density from the climb of edge dislocations, consider in Fig. 2 a bowed-out dislocation segment pinned at two centers separated by a distance ℓ, the mesh length. To remain pinned under a current of point defects constant along the arc, the point defects must pipe-diffuse towards the center of the arc. It is assumed that pipe-diffusion can occur readily such that the dislocation segment always maintains its minimum line energy commensurate with the area F required to accommodate the accumulated atoms. The rate of increase for F is given by

$$\frac{dF}{dt} = VL$$

where V is the climb velocity of an unpinned segment and L is the arc length of the bowed-out segment. As the dislocation segment continues to bow-out, it eventually encounters new pinning centers or it annihilates with another edge dislocation segment. When new pinning centers are encountered, the bowed-out segments are subdivided into new segments with an original mesh length of average value ℓ. The process of regeneration repeats itself with each seg-

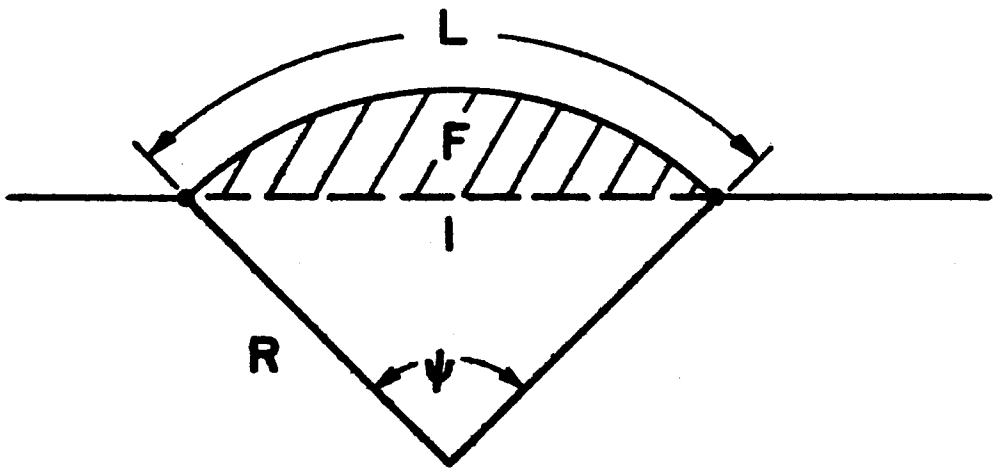

Fig. 2. Geometric parameters for a Bardeen-Herring source.

ment. If τ denotes then the average time of regeneration and L_m the maximum arc length a segment can reach, then the rate of dislocation increase in a volume containing N_d segments is given by

$$B\rho = N_d(L_m - \ell)/\tau \ . \tag{17}$$

The regeneration time may be obtained from

$$\tau = \int_0^{\tau} dt = \frac{1}{V} \int_{\ell}^{L_m} \frac{dF}{dL} \frac{dL}{L} \ . \tag{18}$$

With the help of Fig. 2 it is easy to derive the following geometrical relationships

$$L = \psi \cdot R \ , \qquad \ell = 2R \sin (\psi/2) \tag{19}$$

and

$$F = \frac{1}{2} \left[LR - \ell(R^2 - \ell^2/4)^{1/2}\right] \ . \tag{20}$$

From these it is possible to obtain

$$\tau = \frac{\ell}{2V} \int_0^{\psi_m} \frac{1 - (\psi/2) \operatorname{ctg} (\psi/2)}{\psi \sin (\psi/2)} \, d\psi \ . \tag{21}$$

The dislocation density at any given instant averaged over a sufficiently large volume is given by

$$\rho = \frac{N_s}{L_m - \ell} \int_{\ell}^{L_m} L \, dL \tag{22}$$

if it is assumed that segments bowed out to any length between ℓ and L_m are equally abundant. Equation (22) can also be written as

$$\rho = \frac{N_s}{L_m - \ell} \int L \frac{dL}{d\psi} d\psi = \frac{N_s \ell^2}{L_m - \ell} \int_0^{\psi_m} \frac{\psi^2 [(2/\psi) - \text{ctg } (\psi/2)]}{8 \sin^2 (\psi/2)} d\psi \ .$$

We may use this equation to eliminate the segment density N_s from Eq. (17), use Eq. (21) to eliminate τ, and obtain

$$B\rho = C(L_m/\ell)\ V\rho/\ell \tag{23}$$

where

$$C^{-1}(L_m/\ell) = \left(\frac{\ell}{L_m - \ell}\right)^2 \int_0^{\psi_m} \frac{1 - (\psi/2) \text{ ctg } (\psi/2)}{\psi \sin (\psi/2)} d\psi \int_0^{\psi_m} \frac{[2\psi - \psi^2 \text{ ctg } (\psi/2)]}{8 \sin^2 (\psi/2)} d\psi$$

and $\psi_m = L_m/R(L_m)$. The numerical evaluation of $C(L_m/\ell)$ is shown in Fig. 3. If the segment bows out to a half-circle, then $L_m = \pi\ell/2$, $\psi_m = \pi/2$, and $C(\pi/2) = 1.355$. Except for values of L_m close to ℓ, the coefficient C is of order one, and this approximate value will be used in the following.

In the above derivation, it was also assumed that the climb velocity V of the bowed-out dislocation segment is not dependent on the radius of curvature, R. However, at elevated temperatures when $V_T \cong V_R$, the vacancy concentration in thermodynamic equilibrium with the bowed-out segment is given by [6]

$$C_v^b = C_v^{eq} \exp \left[- \frac{\mu\Omega}{2\pi(1 - \nu)kT} \frac{b}{R} \ln \frac{R}{1.86} \right] , \tag{24}$$

when the bow-out is due to excess interstitial absorption. For the case of

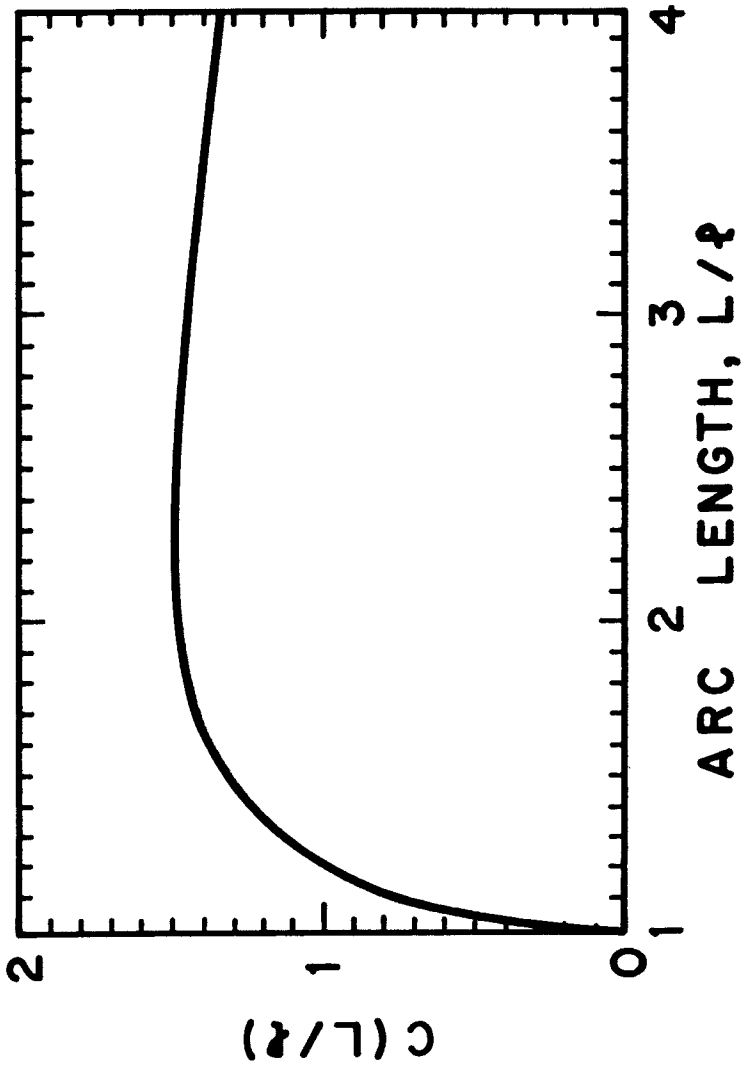

Fig. 3. Coefficient for dislocation generation.

excess vacancy absorption, the sign in the exponential is reversed. Figure 4 shows the ratio C_v^b/C_v^{eq} evaluated for nickel according to Eq. (24). It is seen that $C_v^b - C_v^{eq}$ becomes increasingly negative as R decreases. As a result, the current of thermal vacancies to the bowed-out segment may cancel the excess interstitial flow at elevated temperatures, and the net climb velocity becomes zero. The minimum value of C_v^b is reached when $R = \ell/2$ corresponding to a "minimum" climb velocity of

$$V_m = V_R + V_T \left\{\exp\left[-\frac{\mu\Omega}{\pi(1-\nu)kT}\frac{b}{\ell}\ln\frac{\ell}{3.6\ b}\right] - 1\right\} . \qquad (25)$$

If this climb velocity is zero or negative, the dislocation generation by the Bardeen-Herring process is no longer possible and B = 0.

Accordingly, the rate of dislocation generation is approximately given by

$$B\rho = \begin{cases} \rho V_m/\ell & \text{for } V_m > 0 \\ 0 & \text{for } V_m < 0 . \end{cases} \qquad (26)$$

In the low temperature ($\lesssim 300°C$) range where loops contribute significantly to the dislocation density, the rate of dislocation generation is seen to be given by similar expressions, i.e. by Eqs. (16) and (26). The major difference lies merely in the characteristic length parameters, the average loop radius, $\bar{R}$, in the case of loops, and the average distance between pinning obstacles, ℓ, in the case of network dislocations.

4. BIAS VARIANCE

The radiation-induced part of the climb velocity, V_R in Eq. (10), is proportional to the net bias parameter $(Z_i^d/Z_v^d) - (\bar{Z}_i/\bar{Z}_v)$. It is already

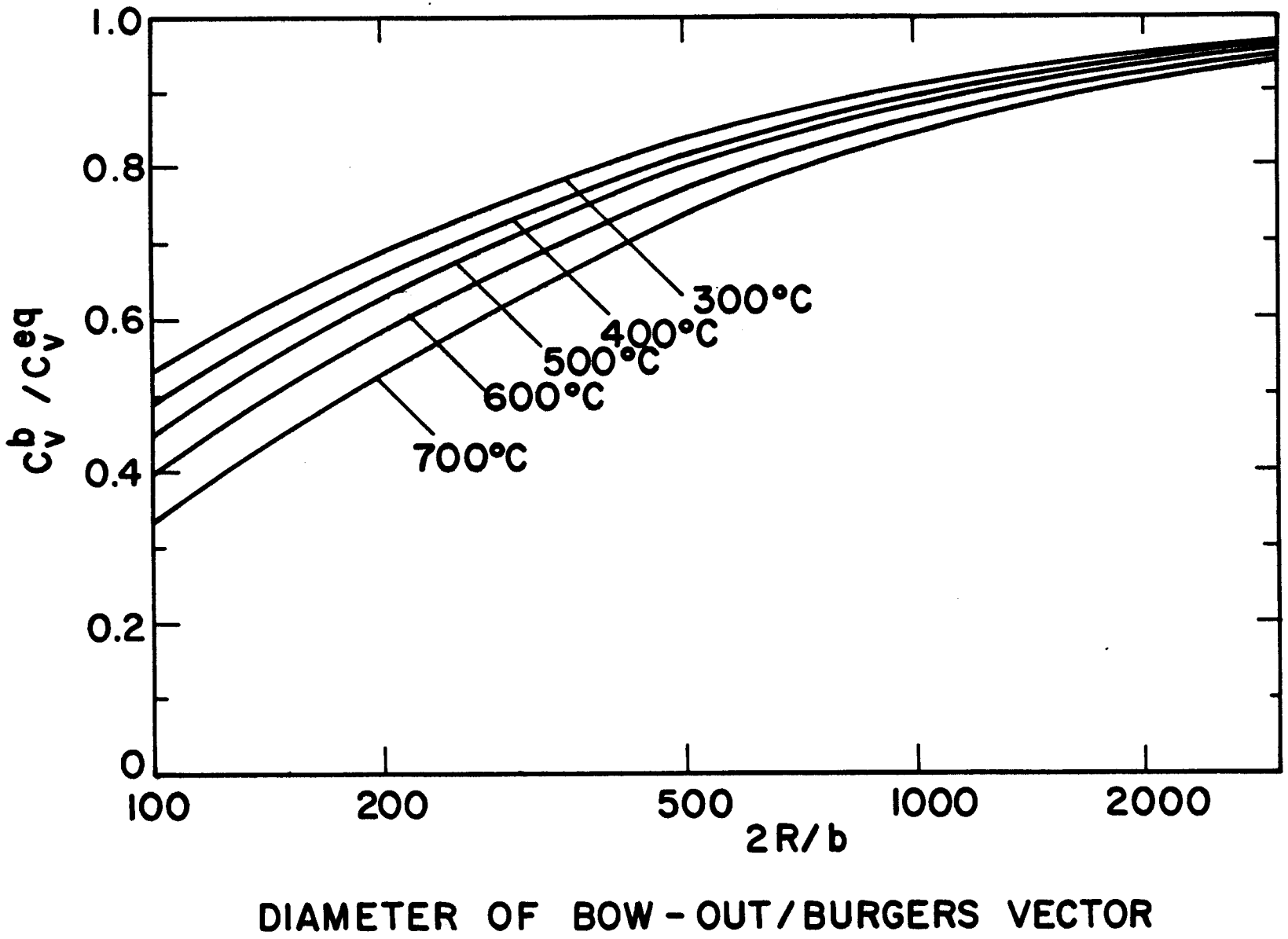

Fig. 4. Ratio of vacancy concentrations in equilibrium with an interstitial dislocation loop and with a straight edge dislocation.

mentioned in Section 2, that this parameter vanishes if only one type of sink is present.

In cold-worked steels, void formation is suppressed for an extended period of irradiation. Nevertheless, during this period the dislocation density has been observed to change dramatically even at temperatures where V_T is negligibly small. It can therefore be concluded that V_R does not vanish even though the net bias is zero when only dislocations are present as sinks.

This paradox can be resolved by taking into account the bias variance of edge dislocations. This variance arises from the partial cancellation of the long-range stress fields of individual dislocations when they are arranged in dense groups. The bias of an individual edge dislocation depends to some degree on the proximity of other edge dislocations and on the directions of their Burgers vector. Wolfer et al. [8] have estimated this bias variance by considering narrowly-spaced dislocation multipoles. They found that the bias of an edge dislocation dipole can be as low as half the value for an isolated edge dislocation, and that dislocations in higher-order multiple configurations have even lower bias values. To take into account this bias variance, we assign the net bias

$$(1 + z)\,\frac{Z_i^d}{Z_v^d} - \frac{\bar{Z}_i}{\bar{Z}_v}$$

to the individual edge dislocation and assume that z is a normally distributed random variable. Then, the average climb velocity V_R remains proportional to $(Z_i^d/Z_v^d - \bar{Z}_i/\bar{Z}_v)$, but Z_i^d and Z_v^d are to be interpreted as mean values for the dislocation bias factors. Furthermore, both positive and negative climb directions contribute to the average climb velocity V_R. However, with regard to

increasing the dislocation line length through climb or with regard to annihilation, the direction of climb does not matter, and we must therefore take the average of the absolute climb velocities. This average is given by integrating over the assumed normal distribution for the bias variance with the result

$$\bar{V}_R = \frac{\Omega}{b} Z_v^d D_v \Delta C_v \int_{-\infty}^{+\infty} dz \left| \frac{Z_i^d}{Z_v^d}(1+z) - \frac{\bar{Z}_i}{\bar{Z}_v} \right| (\sqrt{2\pi}\,\zeta)^{-1} \exp\left(-z^2/2\zeta^2\right)$$

$$= \frac{\Omega}{b} Z_v^d D_v \Delta C_v \left| \frac{Z_i^d}{Z_v^d}\left(1 + \zeta\sqrt{2\pi}\right) - \frac{\bar{Z}_i}{\bar{Z}_d} \right| \qquad (27)$$

$\bar{V}_R$ is to be substituted for V_R in both Eq. (25) and Eq. (16).

The standard deviation, ζ, of the dislocation bias is expected to depend on the dislocation density itself. In a well-annealed material, most dislocations in narrowly-spaced dipole configurations have been annihilated by the very process described in Section 2. The remaining edge dislocations then possess the full bias of an isolated dislocation, and ζ is close to zero. In contrast, in a heavily cold-worked material, many dislocations are part of dense tangles, resulting in a large bias variance. If we assume for this case that $\zeta \cong 1/2$, and $\zeta \cong 0$ for the annealed case,

$$\zeta = 0.5[1 - \exp(-\lambda\rho)] \qquad (28)$$

will provide a plausible dependence of the bias variance on the dislocation density. The choice of $\lambda = 10^{-15}$ cm^2 assures that the bias variance becomes negligible for $\rho \lesssim 10^{15}$ m^{-2}, but approaches its maximum value for $\rho \gtrsim 10^{16}$ m^{-2}.

5. RESULTS AND DISCUSSION

The following predictions for the evolution of the network dislocation density are carried out for 316 austenitic stainless steel. The dislocation bias factors Z_i^d and Z_v^d are evaluated with the formulae given by Sniegowski and Wolfer [9]. Properties used are listed in Table 1. With the exception of the mesh length, all other properties in Table 1 are based on measured or theoretically determined values. The mesh length was selected such that the saturation dislocation density will be 6×10^{14} m^{-2} for an irradiation temperature of 500°C; this density corresponds to experimentally observed saturation densities at about 500°C. The average point defect concentrations produced during irradiation are evaluated with rate theory as outlined in the Appendix. A density of cavity embryos is assumed to exist from the beginning. The density of cavities depends on temperatures and is assumed to be equal to the terminal void number density as observed experimentally. These cavities are allowed to grow according to rate theory which results in void swelling and an increase in the cavity sink strength.

The saturation dislocation density is found to be independent of temperature between 300 and 500°C, but begins to decrease with increasing temperature above about 550°C. Figure 5 shows the dislocation saturation density as a function of temperature for two different mesh length assumptions. The theoretical predictions compare quite well with observed experimental densities [4] as shown in the figure; error bars are shown when given in the references. As can be seen the error in experimental measurement can be quite large. The reasons for the decrease in saturation density as temperature increases is the increasing contribution of thermally induced climb as self-diffusion becomes important. The thermally induced climb is of course responsible for the high

Table 1. Materials Parameters

Parameter	316 Austenitic Stainless Steel
Displacement rate, dpa/s	10^{-6}
Cascade efficiency	0.1
Lattice parameter, a_o, nm	0.3639
Burgers vector, nm	0.2573
Shear modulus, GPa	82.95
Poisson's ratio	0.264
Vacancy migration energy, J	1.92×10^{-19}
Vacancy formation energy, J	2.88×10^{-19}
Pre-exponential factor D_v^o, m^2/s	1.29×10^{-6}
Vacancy relaxation volume, Ω	-0.2
Interstitial relaxation volume, Ω	1.5
Vacancy shear polarizability, J	-2.4×10^{-18}
Interstitial shear polarizability, J	-2.535×10^{-17}
Initial dislocation densities, m^{-2}	
for annealed	4×10^{12}
for cold-worked	7×10^{15}
Mesh length ℓ, μm	0.4

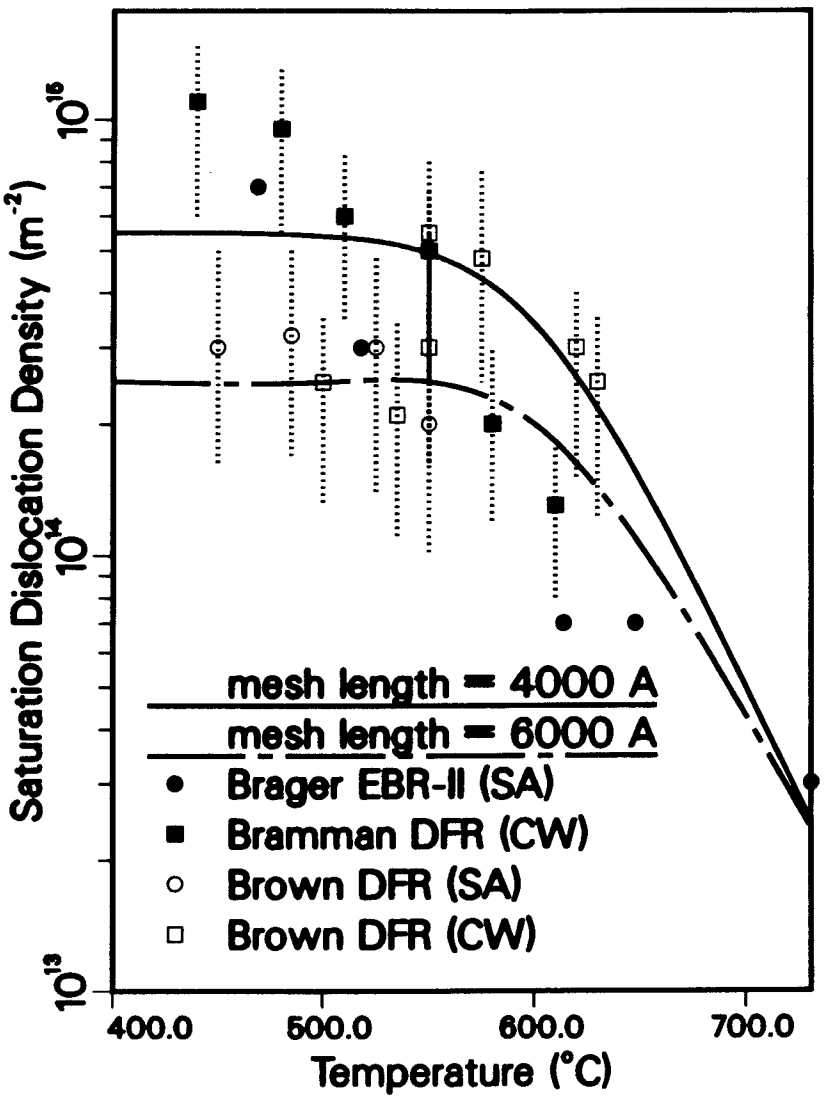

Fig. 5. Saturation dislocation densities in type 316 stainless steel irradiated to doses greater than 20 dpa in breeder reactors.

temperature recovery of cold-worked materials. This recovery can also be described with the present theory by turning off the point defect production rate. Figure 6 shows the results for thermal recovery of the dislocation density in cold-worked 316 austenitic stainless steel. It is seen that the dislocation recovers to a value of 5×10^{13} m^{-2}, typical of solution-annealed material, within about 12 days at an annealing temperature of 700°C. Annealing also occurs at 600°C; but it becomes increasingly insignificant at lower temperatures. These predictions are in general agreement with observation, though no dislocation density measurements have been found in the literature.

Figures 7 and 8 show the predictions for the dislocation evolution for 316 austenitic stainless steel. The time evolution is given in units of dpa, where the dpa rate is 1×10^{-6} dpa/s. The helium/dpa ratio of 0.6 appm He/dpa is typical of fission reactors. The amount of helium in the cavities influences the incubation period before the onset of swelling. Comparison to experimentally measured dislocation densities [4] in the transient region is also shown in the figures and agrees quite well considering the uncertainty in the experimental measurements.

The model developed for the evolution of the network dislocation density reproduces the experimental observations remarkably well. This is significant for two major reasons. First, the materials parameters required are very fundamental and reasonably well known in the case of 316 stainless steels. Therefore, with the exception of the mesh length parameter ℓ and the bias variance ζ, no other parameters required adjustments. The value chosen for ℓ, namely 400 nm, is also reasonably close to the mesh length of bowed-out dislocations observed in micrographs of irradiated steels.

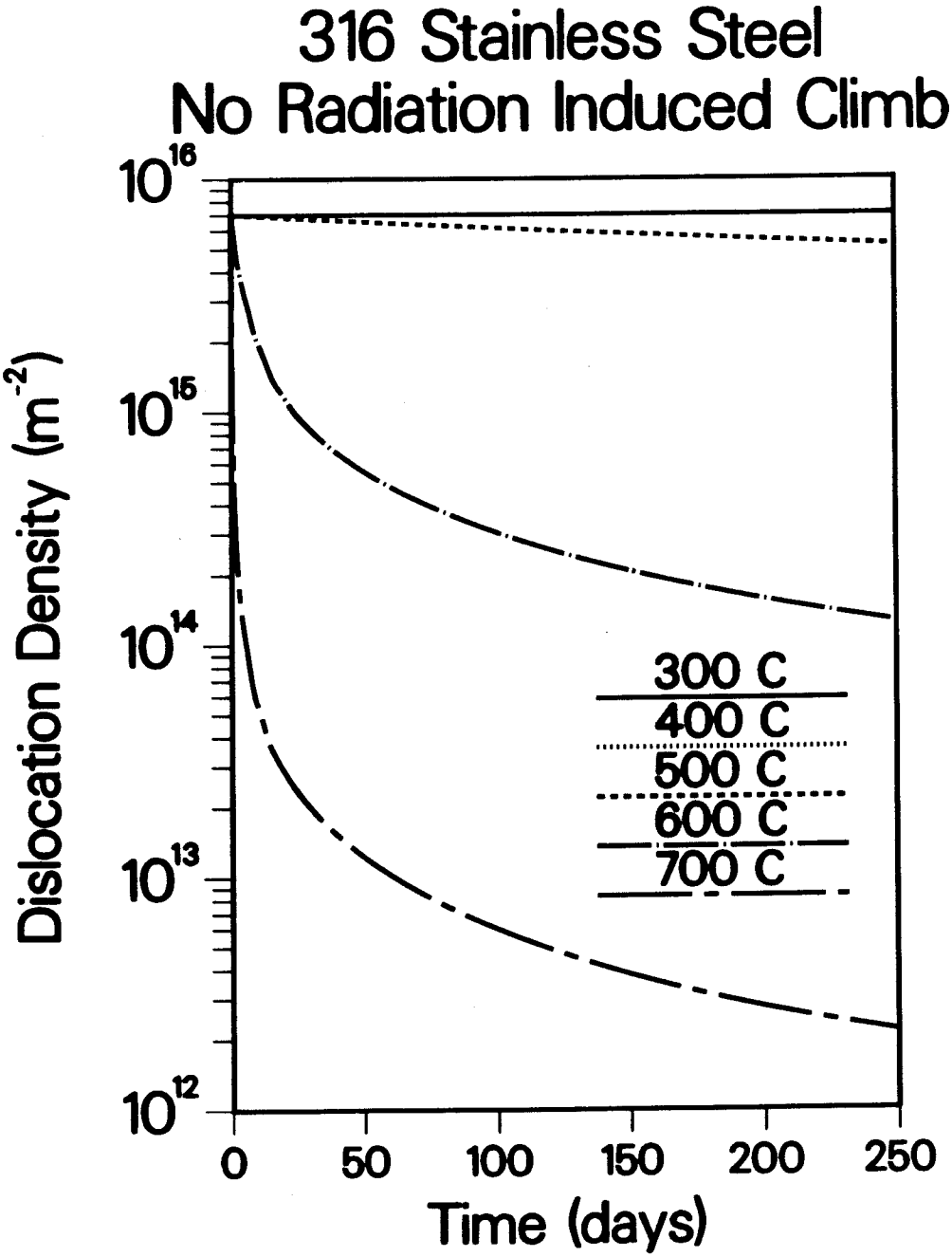

Fig. 6. Predicted recovery of the dislocation density in initially cold-worked 316 stainless steel due to thermal annealing.

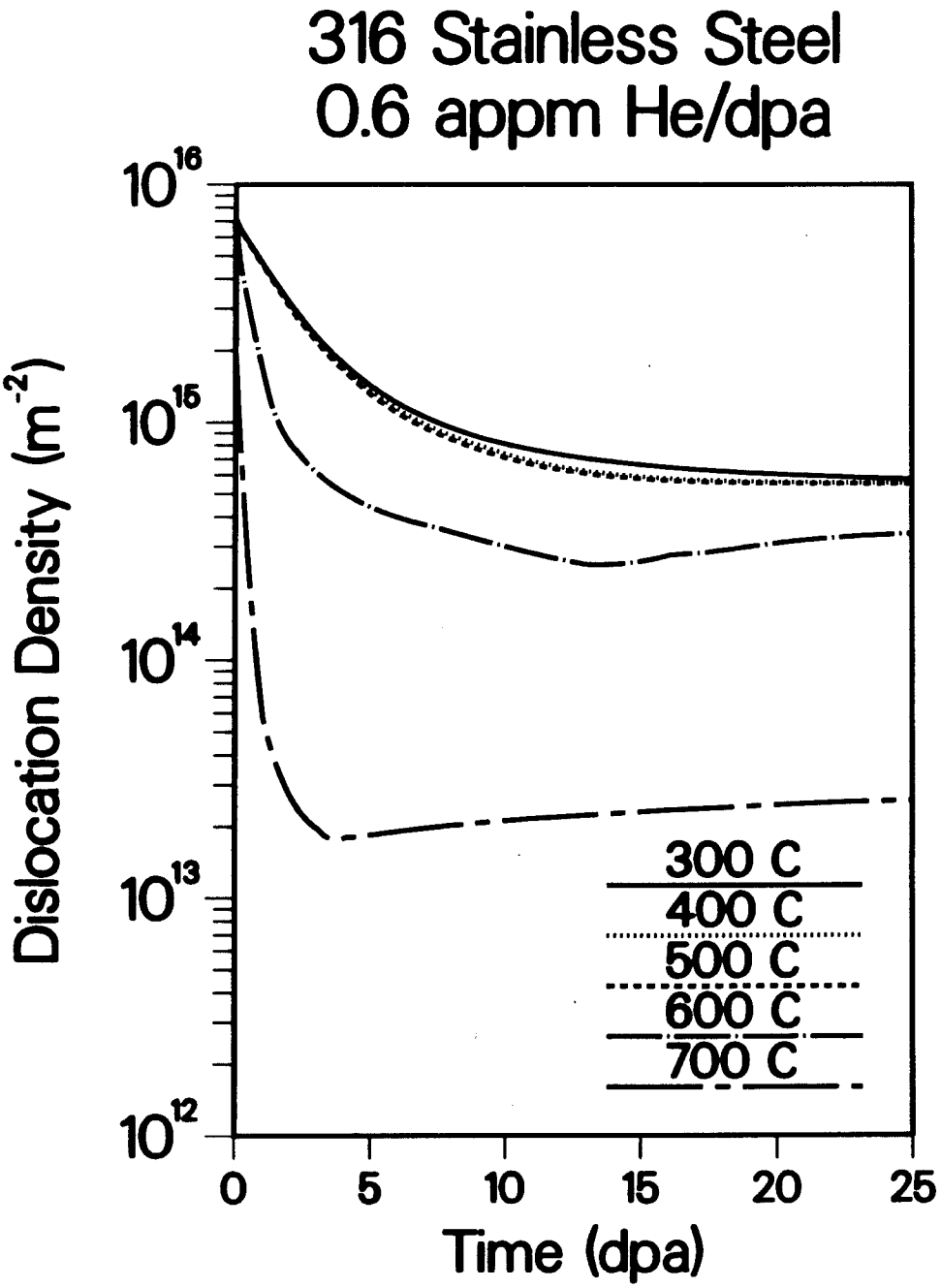

Fig. 7. Dislocation density evolution with irradiation time for cold-worked 316 stainless steel at a displacement rate of 10^{-6} dpa/s.

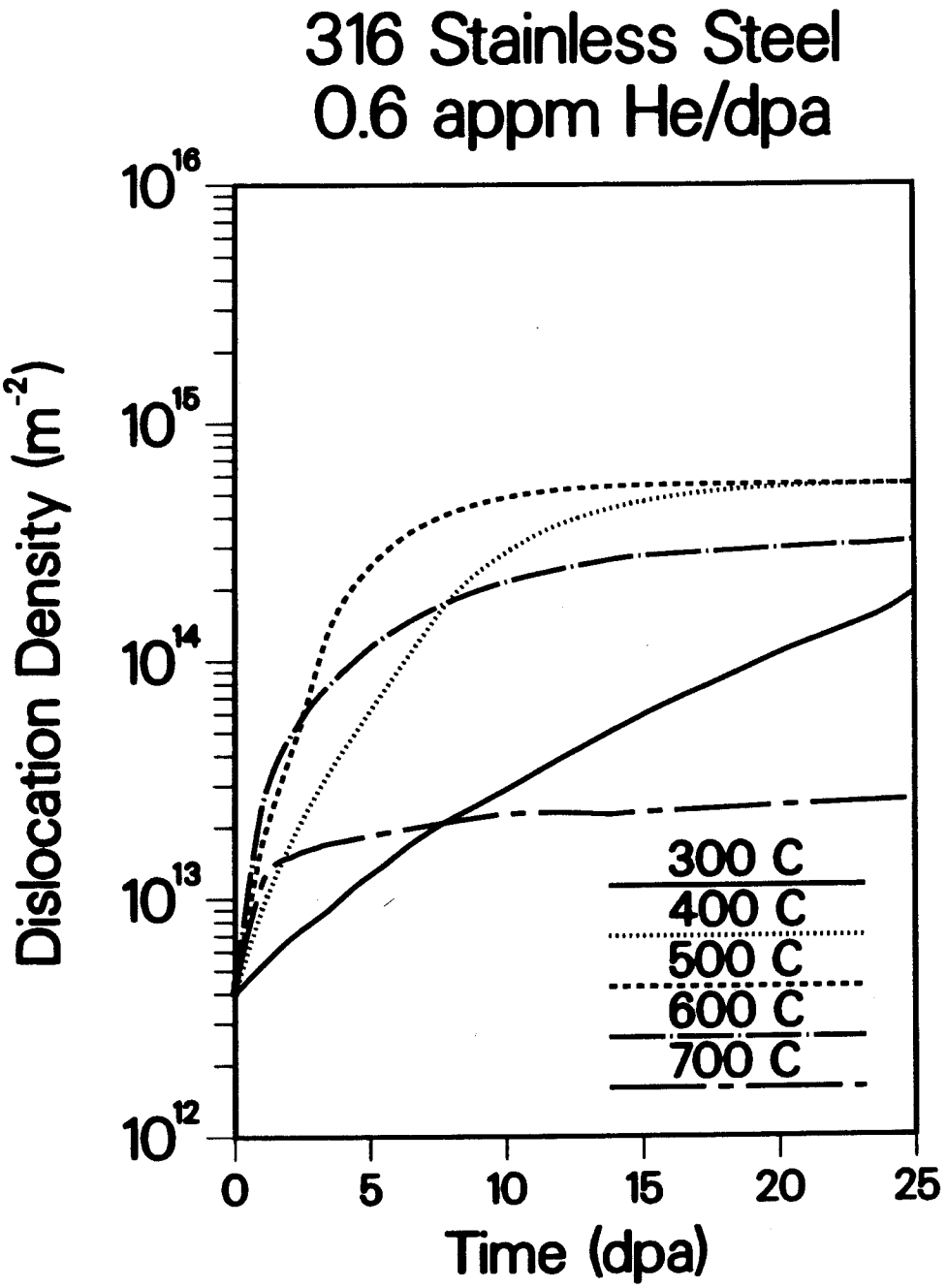

Fig. 8. Dislocation density evolution with irradiation time for solution-annealed 316 stainless steel at a displacement rate of 10^{-6} dpa/s.

The second important implication of the successful model is that the complex dislocation structure and its evolution can in fact be understood in terms of two simple processes: the Bardeen-Herring process of climb in a material with supersaturation of point defects; and the climb-induced annihilation of dislocation dipoles.

The fact that dislocation loops have not been explicitly considered in the present model constitutes both one of its strengths and its weaknesses. Large loops increase their line length very much like a bowed-out dislocation segment, independent of the presence or absence of a stacking fault. When the stacking fault energy is low, as is the case in type 316 SS, the stacking fault does not contribute significantly to the line tension and to the vacancy concentration C_v^b in Eq. (24). Therefore, dislocation loops and bowed-out edge dislocations can indeed be treated as one at higher temperatures.

However, when dislocation loops are small, it is no longer adequate to model them as edge dislocation segments. In this case, loops and network dislocations must be considered as different sinks, and their evolution will have to be described by different models. Based on experimental observation, the loop density increases and their size decreases with decreasing irradiation temperature. It is therefore expected that small dislocation loops are present in type 316 stainless steel at an irradiation temperature of 300°C, and that these loops make a major contribution to the total dislocation density. Accordingly, the present model should not be applied to the entire dislocation structure in materials containing a high density of small dislocation loops.

REFERENCES

1. H.R. Brager, F.A. Garner, E.R. Gilbert, J.E. Flinn and W.G. Wolfer, Rad. Effects in Breeder Structural Materials (edited by M.L. Bleiberg and J.W. Bennett), p. 727, American Inst. of Mining, Metallurgical and Petroleum Engineers, New York (1977).

2. W.G. Wolfer, J. Nuclear Materials 90, 175 (1980).

3. N. Igata, A. Kohyama and S. Nomura, ASTM STP 725, 627 (1981).

4. F.A. Garner and W.G. Wolfer, ASTM STP 782, 1073 (1982).

5. K. Farrell, N.H. Packan and J.T. Houston, Radiation Effects 62, 39 (1982).

6. J.P. Hirth and J. Lothe, Theory of Dislocations, 2nd Ed., John Wiley and Sons, New York (1982).

7. F. Kroupa, Czech. J. Physics B17, 220 (1967).

8. W.G. Wolfer, M. Ashkin and A. Boltax, ASTM STP 570, 233 (1975).

9. J.J. Sniegowski and W.G. Wolfer, Proc. Topical Conf. on Ferritic Alloys for Use in Nucl. Energy Techn. (edited by J.W. Davis and D.J. Michel), p. 579, The Metallurgical Soc. AIME, Warrendale (1984).

APPENDIX

The average concentrations of vacancies and interstitials, C_v and C_i, in a material subject to a constant rate of generation, P, by a fast neutron flux, are given by the two rate equations

$$P - \kappa D_v C_v D_i C_i - D_i C_i \sum_s N^s A^s Z_i^s = 0 \tag{A.1}$$

$$P - \kappa D_i C_i D_v C_v - D_v \sum_s (C_v - C_v^s) N^s A^s Z_v^s = 0 \tag{A.2}$$

where

$$\kappa = 4\pi r_c \left(\frac{1}{D_v} + \frac{1}{D_i}\right)/\Omega \tag{A.3}$$

is the recombination coefficient and r_c the recombination radius for a Frenkel pair. N^s is the density of sinks of type "s", A^s a geometrical factor characteristic of this sink type, and Z_i^s and Z_v^s are the bias factors of this sink type for interstitial and vacancy absorption, respectively.

The solution of the rate equations for $D_i C_i$ and $D_v C_v$ are

$$D_v C_v = D_v \left(\frac{\bar{Z}_i}{\bar{Z}_v} \Delta C_v + \overline{C_v^{eq}}\right) \tag{A.4}$$

$$D_i C_i = D_v \Delta C_v \tag{A.5}$$

where

$$\bar{Z}_{i,v} = \sum_s N^s A^s Z_{i,v}^s \Big/ \sum_s N^s A^s \tag{A.6}$$

are sink-averaged bias factors and

$$\overline{C_v^{eq}} = \sum_s N^s A^s Z_v^s C_v^s \Big/ \sum_s N^s A^s Z_v^s \qquad (A.7)$$

is the sink-averaged thermal vacancy concentration. The vacancy concentration in local thermodynamic equilibrium with the sink of type "s" is denoted by C_v^s.

The excess vacancy concentration ΔC_v is given by

$$\Delta C_v = \frac{\bar{N}\,\bar{Z}_v}{2\kappa D_v} \{[M^2 + L]^{1/2} - M\} \qquad (A.8)$$

where $$M = 1 + \kappa D_v \overline{C_v^{eq}} \Big/ \bar{N}\,\bar{Z}_i$$

and $$L = 4P\kappa/(\bar{Z}_i \bar{Z}_v \bar{N}^2) .$$

Here, $\bar{N} = \sum_s N_s A_s$ is the total sink strength.